

Ageing durability of SiR under prolonged voltage stress, contaminant flow and contaminant concentration: a statistical approach

Nornazurah Nazir Ali¹, Hidayat Zainuddin¹, Jeefferie Abd Razak², Nur Farhani Ambo³

¹Fakulti Teknologi and Kejuruteraan Elektrik, Universiti Teknikal Malaysia Melaka (UTeM), Melaka, Malaysia

²Fakulti Teknologi and Kejuruteraan Industri and Pembuatan, Universiti Teknikal Malaysia Melaka (UTeM), Melaka, Malaysia

³Fakulti Seni Bina and Kejuruteraan, Universiti Teknologi Kreatif Limkokwing, Cyberjaya, Malaysia

Article Info

Article history:

Received Jan 4, 2024

Revised Mar 21, 2024

Accepted Mar 28, 2024

Keywords:

Contaminant concentration

Flow rate

Leakage current

Optimization

Silicone rubber insulator

ABSTRACT

Silicone rubber (SiR) has become a reliable choice for outdoor high voltage (HV) insulation in recent years. However, the durability of these polymeric materials is affected by both electrical and environmental stresses, leading to aging. While prior research aimed at enhancing performance, little focus was placed on identifying the major root causes of aging in these insulators. To delve into the causes, we conducted inclined plane tracking (IPT) tests, varying voltage, flow rate, and contamination concentration. Samples with consistent alumina trihydrate (ATH) filler content were tested under the BSEN 60587 standard. The voltage ranged from 3.5-5.5 kV, flow rate from 0.3-0.9 ml/min, and contamination concentration from 500-4500 $\mu\text{S}/\text{cm}$. A Two-Level Factorial analysis with a design of experiment (DOE) approach was used. The study revealed that contaminant concentration significantly impacted leakage current (LC), followed by contamination flow rate and voltage. Additionally, optimization techniques are used to determine ideal LC values under specific conditions. This study explains how each factor affects LC values, allowing for predictive modelling, which improves our understanding of SiR insulators' durability, optimizes LC in real-world situations, and improves their performance and lifespan.

This is an open access article under the [CC BY-SA](https://creativecommons.org/licenses/by-sa/4.0/) license.



Corresponding Author:

Hidayat Zainuddin

Fakulti Teknologi and Kejuruteraan Elektrik, Universiti Teknikal Malaysia Melaka (UTeM)

St. Hang Tuah Jaya, 76100 Durian Tunggal, Melaka, Malaysia

Email: hidayat@utem.edu.my

1. INTRODUCTION

Polymeric high voltage (HV) insulators are one of the key components in the transmission and distribution system. Polymeric insulators like silicone rubber (SiR) thrive better than glass and ceramic insulators. Excellent hydrophobicity, lightweight, and high resistance to tracking and erosion are a few advantages of SiR. However, the primary concern of polymeric insulators is their long-term performance in the real environment as harsh weather and pollution can affect the performance of insulators and may cause unplanned line outages [1]. HV insulators need to withstand both electrical and environmental stresses to ensure their reliability in the long run. Exposure to electrical stress (corona and dry band discharges) and environmental stresses (heat, chemicals, salts, and acid) can degrade the polymer, resulting in insulator aging [2], [3].

Previously, it was observed that insulation samples with thicker pollutant layers tended to show higher leakage current (LC) values, though these values may vary due to scintillation [4]. Another study

found that moisture reduced the surface resistance of aged polymeric insulators, significantly increasing LC under wet and polluted conditions [5]. Next, HV insulators exhibited elevated LC values when exposed to marine pollutants, indicating the detrimental impact of salts and water on outdoor insulation [6]. Additionally, rainwater with high anion levels results in lower pH values and increased acidity, impacting conductivity levels and contributing to insulator degradation. In fact, rainwater in certain region regions, such as Bintulu and Kuching, recorded high inorganic content with pH levels ranging from 4.3 to 7 [7]. Urban areas like Kuala Lumpur have slightly acidic rainwater with a pH range of 5.9-6.5 [7], [8]. Besides pollutants, a rise in voltage could also intensify the electric field stress of the tracking test [9]. On the contrary, the tracking resistance of SiR was found to be the lowest at 4.5 kV despite the voltage ranges of 3 to 5 kV [10], implying that increased voltage may not always compromise the material's resilience to tracking and erosion. Therefore, to assess insulator suitability in different environmental conditions, it is crucial to understand how voltage, contaminant levels, and moisture affect the LC intensity of the insulator, as these factors represent some of the stressors present in the real environment of an outdoor insulator.

Recent studies have shown the analysis of the performance of polymers against electrical and environmental stresses, and some have been tested under rapid aging by analyzing their LC [11]–[13]. Rapid aging tests, such as the inclined plane tracking (IPT) test, mimic harsh environments under controlled conditions, enabling researchers to assess an insulator's resistance to environmental and electrical stresses in a shorter time. The LC values provide insights into surface conditions and the connection between electrical discharges, pollution levels, and surface conductivity. Therefore, IPT is a convenient method for monitoring and diagnosing insulator surface conditions [14]. Moreover, it's crucial to identify the optimized factors leading to the lowest LC. In fact, the significance of optimization in today's diverse industries is undeniable [15]–[17]. After careful consideration, this study will unveil the significance of three critical factors (voltage, flow rate, and contaminant concentration) and their interactions in affecting the LC intensity of SiR insulator samples via IPT test. The LC values will be analyzed to obtain the impact of each factor. This research also enables us to gauge the performance of SiR through predictive analysis of the LC values within the chosen ranges of the factors, offering valuable information on factor interaction and optimization of SiR, facilitating decision-making in real-life HV insulator applications.

2. METHOD

This section consists of the sample preparation and experimental setup of the IPT test. The chronological of sample preparations is explained. In addition, the experimental setup details are also provided.

2.1. Samples preparation and experimental setup

The samples of SiR were prepared using raw Elastosil R401 SiR, peroxide curing agent of dicumyl peroxide (DCP) (98% active), alumina trihydrate (ATH) micro filler and heat stabilizer. The mix of SiR samples consists of 50 pphr of ATH, 0.5 pphr of DCP, and 2 pphr of heat stabilizer. The particular combination of SiR blends was chosen based on prior research on SiR with the highest surface resistivity and relative permittivity [18]. Table 1 highlights the samples run and their recorded LC values. For an easy representation of factors, voltage is also labelled as A, flow rate as B, and contamination concentration as C.

Table 1. The experimental conditions are created by varying the values of factors using the software

Run	A (kV)	B (ml/min)	C ($\mu\text{S}/\text{cm}$)	LC values (A)	
				60 minutes	360 minutes
1	5.5	0.9	4500	0.018483	0.045863
2	3.5	0.9	4500	0.0119907	0.028884
3	5.5	0.3	4500	0.0070938	0.018964
4	3.5	0.3	4500	0.0067391	0.0144639
5	5.5	0.9	500	0.0061885	0.01994
6	3.5	0.9	500	0.0008019	0.001033
7	5.5	0.3	500	0.0022849	0.0041148
8	3.5	0.3	500	0.000372	0.0005118
9	4.5	0.6	2500	0.0084544	0.0218242
10	4.5	0.6	2500	0.00720272	0.02322
11	4.5	0.6	2500	0.00804327	0.0192007

The experiment was conducted based on the standard BS EN 60587 IPT test of the constant tracking method. It should be noted that, according to the standard, the LC values should be below 60 mA. The values set for voltage ranges were 3.5 to 5.5 kV, the flow rate 0.3 to 0.9 ml/min, and the contaminant concentration

were 500 to 4500 $\mu\text{S}/\text{cm}$. The experimental conditions of the two factorial methods were decided via Design Expert Software. There is an overall 11 run with three repetitions at a center point. The experimental setup can be reviewed from reference [13]. Then, to allow easy representation of the factors, voltage is labeled as A, flow rate as B, and contaminant concentration as C. The LC values obtained were analyzed based on two stages of analysis. The first stage is at the 60-minute mark, and the second is at the 360-minute mark of the IPT test.

3. RESULTS AND DISCUSSION

The obtained LC values from both stages are compared to see the relations between the increment in LC and the contributions of each factor. The results were analyzed and discussed in subsequent subsections. The subsection comprises contribution level, interaction plot, ANOVA, regression equations, 3D response surface interaction plots, and optimization.

3.1. Contribution percentage of factors affecting LC values

The percentage of contribution indicates the role of each factor and its interaction in influencing the LC values of the tested samples. A statistical comparison was made between each term's contribution percentage at the first and second stages. Table 2 shows both stages' contribution percentages and p-values.

Table 2. The percentage of contributions and p-value for both stages

Term	First stage		Second stage	
	(%) contributions	p-value	(%) contributions	p-value
A: voltage	9.43	0.0159	13.89	0.0168
B: flow rate	20.73	0.0073	23.86	0.0099
C: contaminant concentration	56.60	0.0027	48.93	0.0049
AB	4.35	0.0335	5.54	0.0406
AC	0.0096	0.8254	0.008	0.8747
BC	7.14	0.0208	4.48	0.0495
ABC	0.33	0.2779	0.06	0.6729
Overall model	-	0.0108	-	0.0171

In both stages, the primary factor influencing the LC values was C, accounting for 56.6% in the initial stage and 48.93% in the second stage. B was the second most significant factor in both stages, contributing 20.73% and 23.86%, respectively. Factor A followed by 9.43% in the first stage and 13.89% in the second stage. Next, for the interaction between these factors, AB recorded 4.35% in the initial stage and 5.54% in the second stage, while BC was 7.14% and 4.48%, respectively. However, the AC factor is the most minimal. Previous electrical failure simulations reported an increase in current density with rising contaminant flow rate and voltage. However, there was no analysis on contaminant concentration or factor interactions [19].

3.2. Analysis of variance

Analysis of variance (ANOVA) analysis emphasizes the significance of factors affecting the LC values for SiR samples via p-value, as shown in Table 2. An element is deemed significant if the p-value is ≤ 0.05 and insignificant if ≥ 0.10 . In statistics, the coefficient of determination (R^2) measures how well the model replicated the outcomes or regression model, with one as the best value. In this case, the LC at the first and second stages is the dependent variable, while the A, B, and C factors are independent variables. The overall model for both stages show a significant p-value of 0.0108 in the first stage and 0.0171 in the second stage, with an R^2 value of 0.9969 for the first stage and 0.9951 for the second stage, indicating high accuracy for the model. The p-values of A, B, C, AB, and BC are significant in both stages, with values ≤ 0.05 . The high contribution percentages of the single factors A, B, and C are not shocking as these results are aligned with the fundamental process of tracking and erosions, which begins when samples are exposed to the contaminant. The presence of LC across the insulator induces ohmic heating, leading to the formation of dry band arcing (DBA), damaging the surface hydrophobicity and exacerbates LC across the exposed area. Hence, thermal depolymerization and deterioration of the polymeric samples become inevitable [9]. It should be noted that the interactions between factors can be complex and non-linear, and their combined effects may not always be straightforward.

3.3. Interaction plot

The interaction plot provides insights into the relationship between two independent factors, uncovering causal connections where changes in one factor directly influence the other, shedding light on

their mutual reliance and interdependency. The plots can also reveal interaction effects between the two factors based on the third factor. Unveiling hidden trends that may not be evident when studying each factor individually.

3.3.1. The first stage

The interaction plot between factors A and B is presented in Figure 1. An increase in factor A is followed by an increase in LC values for both concentrations of B (0.3 and 0.9 ml/min). In Figure 1(a), the red line representing B at 0.9 ml/min increases by 5.39 mA as A increases from 3.5 to 5.5 kV. For B at 0.3 ml/min, the LC increases by only 1.91 mA. In Figure 1(b), an increase in A results in a rise of 6.5 mA in LC for B at 0.9 ml/min and an insignificant rise of 0.36 mA for B at 0.3 ml/min. In both figures, LC values increase more prominently for B at 0.9 ml/min. LC also increases as C rises from 500 to 4500 $\mu\text{S}/\text{cm}$. Specifically, at 3.5 kV, the LC for B at 0.9 ml/min increases by 11.19 mA; at 5.5 kV, it increases by 12.3 mA. Conversely, the increases are lower for B at 0.3 ml/min (6.47 mA at 3.5 kV and 4.8 mA at 5.5 kV). In this stage, factor A strongly affects LC values for B at 0.9 ml/min. The increase in LC is intensified by the rise in factor C, highlighting the impact of higher contaminants on the LC values. Perhaps an increase in C induces higher conductivity levels, as it has previously been found that acidity (pH value) could impact the conductivity levels of rainwater [9].

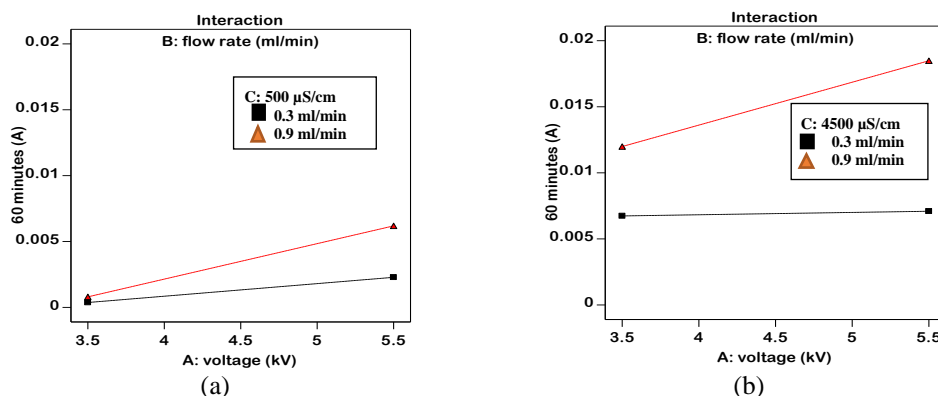


Figure 1. Interaction between A and B when; (a) C at 500 $\mu\text{S}/\text{cm}$ and (b) C at 4500 $\mu\text{S}/\text{cm}$ at 60 minutes

Next, exploring the relations of BC with 7.14% of the contribution is also essential. The interaction between factors B and C is shown in Figure 2. In Figure 2, as B increases, the LC also increases. In Figure 2(a), for C at 4500 $\mu\text{S}/\text{cm}$, LC increases by 5.25 mA as B rises from 0.3 to 0.9 ml/min, but for C at 500 $\mu\text{S}/\text{cm}$, the increase in LC increases is merely by 0.43 mA. Similarly, for Figure 2(b), as B increases, C at 4500 $\mu\text{S}/\text{cm}$ exhibits a higher rise in LC at 11.39 mA, while for C at 500 $\mu\text{S}/\text{cm}$, the surge was at 3.9 mA. In both figures, the rise in LC values was more noticeable for the higher value of C (4500 $\mu\text{S}/\text{cm}$). In both Figures, the elevation of A from 3.5 to 5.5 kV led to a rise in LC. Specifically, at 0.3 ml/min, LC increases by 0.35 mA for C at 4500 $\mu\text{S}/\text{cm}$ and 1.9 mA for 500 $\mu\text{S}/\text{cm}$. At 0.9 ml/min, C at 4500 $\mu\text{S}/\text{cm}$ exhibited a 6.5 mA increase, whereas at 500 $\mu\text{S}/\text{cm}$, the rise was 5.3 mA. B majorly affects LC values for C at 4500 $\mu\text{S}/\text{cm}$. However, for 500 $\mu\text{S}/\text{cm}$, the impact of B is less prominent. In this first stage, factor C is more influential in affecting overall LC increment, matching the highest percentage of contributions, as shown in Table 2. Comparing the LC trends in Figures 1(b) and 2(b) reveals a more pronounced rise of LC in 2(b), aligning with a higher percentage of contribution for BC than AB at this stage.

3.3.2. The second stage

The interaction plot between factors A and B is presented in the following Figure 3. Increasing A leads to a rise in LC values for factor B with both concentrations. In Figure 3(a), as A increases from 3.5 to 5.5 kV, B at 0.9 ml/min shows an increase of 18.91 mA in LC, while B at 0.3 ml/min shows a rise of 3.6 mA. Likewise, as in Figure 3(b), as A rises, the LC for B at 0.9 ml/min increases by 16.98 mA, while for B at 0.3 ml/min, the rise is only by 4.5 mA. LC also increases as C rises from 500 to 4500 $\mu\text{S}/\text{cm}$. Specifically, at 3.5 kV, the LC for B at 0.9 ml/min increases by 27.85 mA; at 5.5 kV, it increases by 25.92 mA. The increments are lower for B at 0.3 ml/min with 13.95 mA at 3.5 kV and 14.85 mA at 5.5 kV. Upon comparison, Figures 3(a) and (b) show a notable influence of factor A on the increase in LC for B,

particularly at 0.9 ml/min and especially when C is 4500 $\mu\text{S}/\text{cm}$. Compared to the first stage, the rate of overall LC increment also appears to be more pronounced for 0.3 ml/min, accounting for the rise in the contribution percentage of AB by 1.19, A by 4.46%, and B by 3.13%.

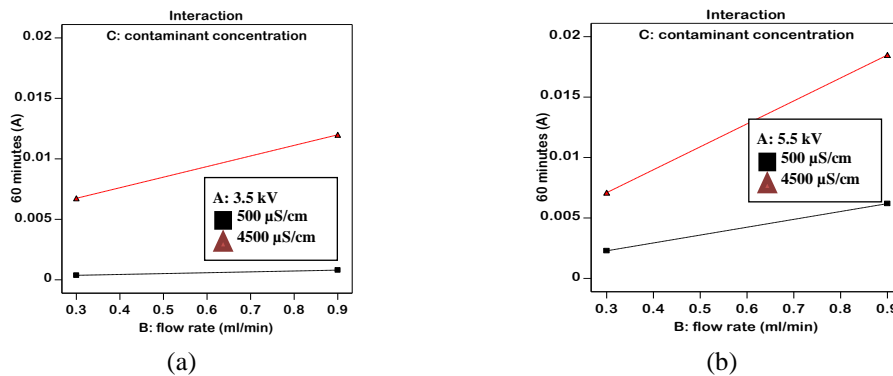


Figure 2. Interaction between B and C when; (a) A at 3.5 kV and (b) C at 5.5 kV at 60 minutes

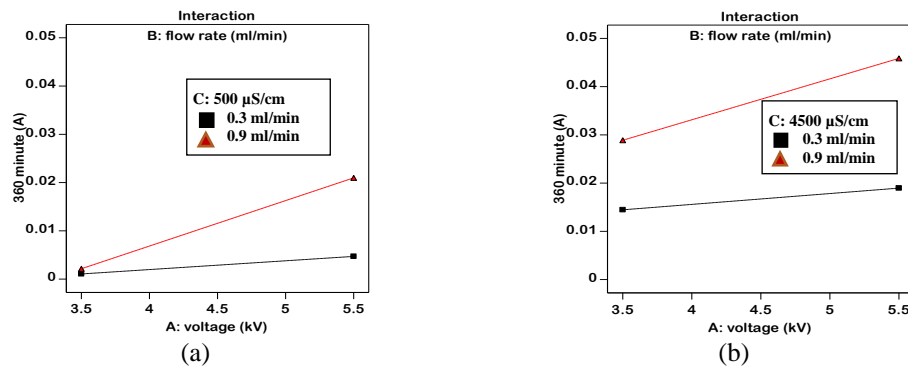


Figure 3. Interaction between A and B when; (a) C at 500 $\mu\text{S}/\text{cm}$ and (b) C at 4500 $\mu\text{S}/\text{cm}$ at 360 minutes

In Figure 4(a), for C at 4500 $\mu\text{S}/\text{cm}$, LC increases by 14.42 mA as B escalates from 0.3 to 0.9 ml/min. As for C at 500 $\mu\text{S}/\text{cm}$, the upswing in LC amounts to a mere 0.52 mA. In Figure 4(b), the rise of B leads to a more substantial boost in LC for C at 4500 $\mu\text{S}/\text{cm}$, increasing by 26.9 mA. Conversely, C at 500 $\mu\text{S}/\text{cm}$ had a rise of 15.83 mA. In this stage, the effect of B becomes more pronounced for C at 500 $\mu\text{S}/\text{cm}$, mainly when A is set at 5.5 kV. This could be due to the rise in the percentage of contribution of factor A at this stage.

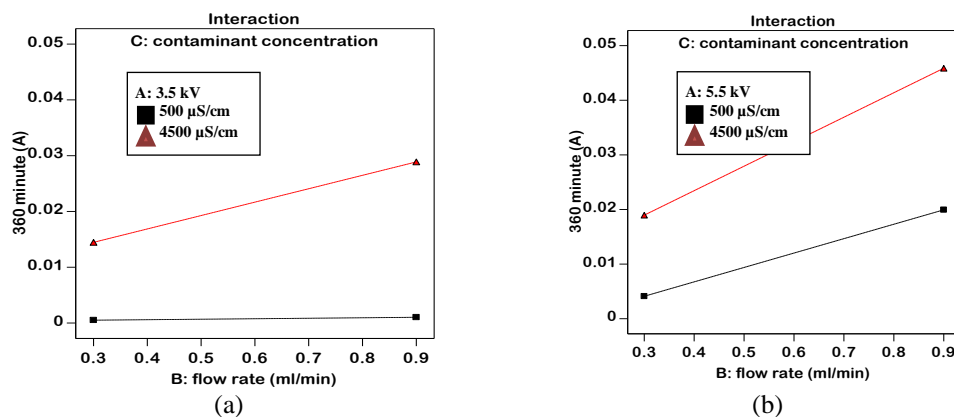


Figure 4. Interaction between B and C when; (a) A at 3.5 kV and (b) C at 5.5 kV at 360 minutes

3.4. Regression equation

The regression equation can be utilized for predictive analysis. The prediction of LC values can be made by substituting the original unit values for the factors. In (1) depicts the regression equation for the first stage and (2) for the subsequent stage. The equation visualizes the relationship between the input and response variables, enabling LC estimation for improved SiR insulator performance and longevity in real-life conditions.

$$\begin{aligned} \text{first stage} = & 0.000888 - 0.000307A - 0.015447B + 1.27776 \times 10^{-6}C + 0.004262AB \\ & - 8.7775 \times 10^{-8}AC + 2.27081 \times 10^{-6}BC - 1.19542 \times 10^{-7}ABC \end{aligned} \quad (1)$$

$$\begin{aligned} \text{second stage} = & 0.008418 - 0.00265A - 0.05083B - 2.39247 \times 10^{-7}C + 0.01416AB \\ & + 5.98681 \times 10^{-7}AC + 9.90014 \times 10^{-6}BC - 1.25215 \times 10^{-6}ABC \end{aligned} \quad (2)$$

3.5. The 3D response surface plots

The 3D-response surface plots allow a clearer view of the interactions between all independent factors, visualizing the relationship between multiple factors and the response variable. The 3D representation of the AB and BC interaction is discussed in which the x and y-axis represent the factor while the z-axis represents the LC.

3.5.1. The first stage

Figure 5(a) depicts the 3D interaction of factors A and B, while Figure 5(b) illustrates the 3D interaction of B and C. The highest LC value of AB interaction is 12.2276 mA, while for BC, it is 15.1241 mA. At this stage, factors B and C appear to contribute to the LC increment. The heightened LC value for BC in this stage supports the rationale for its greater contribution percentages compared to AB. Earlier, R. Hackam elucidated that transient hydrophobicity loss due to moisture is minimal but could notably accelerate when caused by contamination-induced hysteresis [20], [21]. As hydrophobicity wanes, tracking and erosion are triggered, which explains why the BC interactions were more pronounced than those involving other factors in the initial phase of the IPT test.

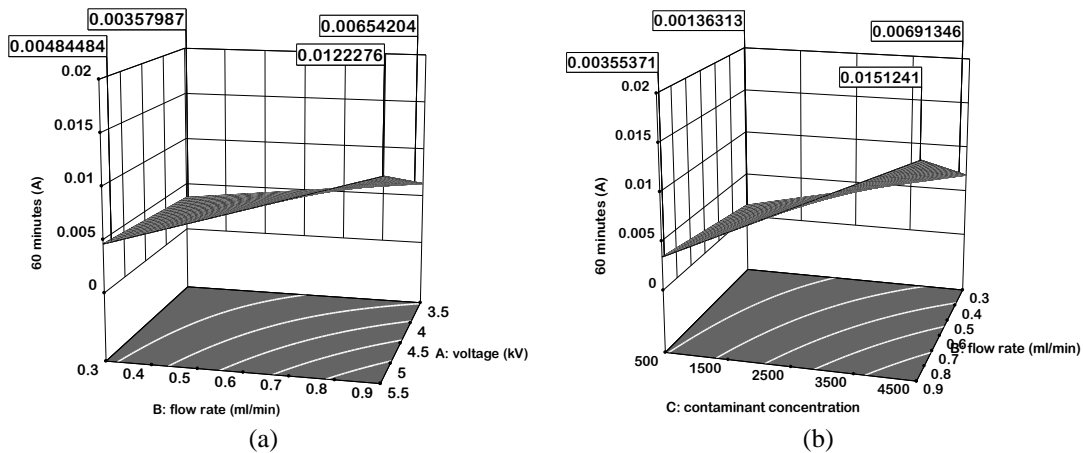


Figure 5. The 3D-response surface plot between; (a) A and B factors when C remained constant and (b) B and C factors when A remained constant

3.5.2. The second stage

Figure 6(a) depicts the 3D interaction of factors A and B, while Figure 6(b) illustrates the 3D interaction of B and C. In this stage, the highest peak of AB interaction is 32.76 mA, while for BC, it is 37.24 mA. Notably, this stage illustrates a noticeable increase in the overall LC values compared to the first stage. The LC peak of AB surged by 167.51%, while BC rose by 145.83%. The increase in the test time led to more hydrophobicity loss, intensifying samples' LC and aging. Therefore, aged insulators usually had a higher LC value [22].

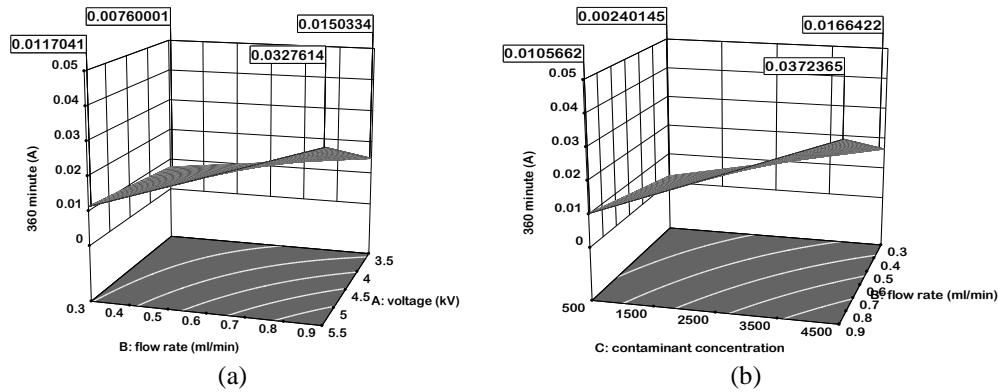


Figure 6. The 3D-response surface plot between; (a) A and B factors when C remains constant and (b) B and C factors as A remained constant

3.6. The optimization and process capability index (Cpk) for SiR samples

Optimization is only performed on the LC data for the second stage, a critical stage that describes the tolerance LC for the samples. This part deduces combinations at factor levels that satisfy all specifications on each factor while maintaining an output with high process capability index (Cpk) and desirability values. Desirability values help find the best factor settings that meet specific target goals for multiple response variables [23]. Cpk is a statistical measure that evaluates a process's ability to produce output within set limits. The Cpk value ranges from 0 to 1 or higher and can vary according to industry standards and needs. The commonly used guidelines: $Cpk < 1$: the process is incapable of meeting the specifications; $1 \leq Cpk < 1.33$: the process is slightly capable and needs improvement to comply with specifications; $1.33 \leq Cpk < 1.67$: the process is competent and consistent in meeting specifications; $1.67 \leq Cpk < 2$: very capable, well within limits and high level of consistency; $Cpk \geq 2$: a robust process with minimal variability [24], [25]. Figure 7 shows the optimization under a few conditions.

In Figure 7(a), A was set to a maximum and BC to a minimum, and the achievable LC is 9.69479 mA with Cpk of 1.5 and desirability of 93.3 %. In Figure 7(b), only B was set to a maximum, and the achievable LC is 9.69481 mA with a Cpk of 1.5 and desirability of 93.3%. In Figure 7(c), only C was set to maximum, and the LC is 14.4639 mA with 100% desirability and 2.28 of Cpk. In Figure 7(d), all factors were set to a maximum, and the predicted LC is 36.68 mA, with Cpk of 1.5 and 92.8% desirability. Overall, the values of LC get more intense as the factor maximizes. However, obtaining samples with low LC, high accuracy and high desirability is feasible by comprehending the connections between factors and applying the appropriate optimization strategies.

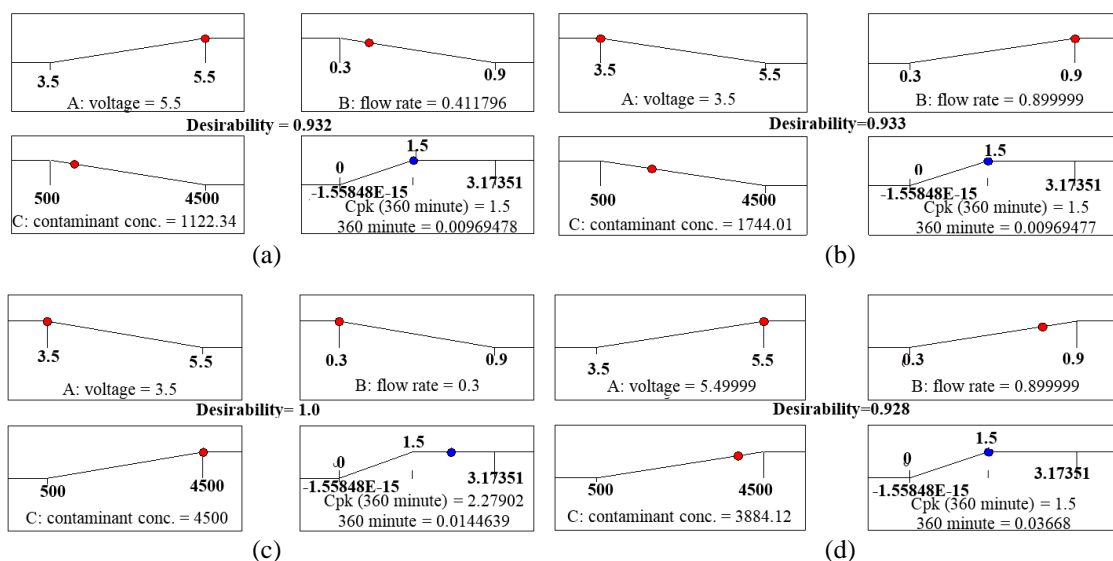


Figure 7. Optimization of factors value to get minimum LC via; (a) maximum A, minimum B and C; (b) maximum B, minimum C and A; (c) maximum C, minimum A and B; and (d) maximum A, B, and C

4. CONCLUSION

In conclusion, the study successfully evaluated the impact of voltage (A), flow rate (B), and contamination concentration (C) on the leakage current (LC) values of SiR for failure analysis. Contamination concentration had the most significant impact on LC values, followed by flow rate and voltage. Interactions between factors AB and BC also contributed to increased LC intensity. The predictive equation for LC values under varying conditions was deduced, and 3D-response surface plots and optimization provided a precise evaluation of the contributions and impacts of all factors and their interactions. The SiR samples demonstrated the ability to withstand all tested conditions, with the highest LC score well below the 60 mA threshold allowed during the IPT test. This study highlights the SiR blends' capacity to endure various factors and optimize LC outcomes, offering insights into producing more competent and consistent insulating materials. The findings not only reveal the roles and interactions of each factor in affecting LC values and SiR insulator failure but also predict the SiR insulator's producibility and resilience in real-world environments.

ACKNOWLEDGEMENTS

The authors wish to extend their utmost appreciation to the Universiti Teknikal Malaysia Melaka (UTeM) for the support of facilities provided during the research. An expression of gratitude is also given to Immortal Green Industrial Sdn. Bhd. for the research materials support.




REFERENCES

- [1] M. G. Shaik and V. Karupaiyan, "Effect of ageing on the tracking characteristics of high-temperature vulcanized silicone rubber hybrid composites for HV insulation," *Materials*, vol. 13, no. 10, May 2020, doi: 10.3390/ma13102242.
- [2] B. Allen, M. Bleszynski, M. Kumosa, and E. Willis, "Investigation into the effects of environmental stresses on RTV-1 silicone-based caulk materials," *IEEE Transactions on Dielectrics and Electrical Insulation*, vol. 22, no. 5, pp. 2978–2986, 2015, doi: 10.1109/TDEI.2015.004795.
- [3] H. de Santos and M. SanzBobi, "Research on the pollution performance and degradation of superhydrophobic nano-coatings for toughened glass insulators," *Electric Power Systems Research*, vol. 191, 2021, doi: 10.1016/j.epsr.2020.106863.
- [4] N. S. Sunitha, R. Prakash, and K. N. Ravi, "Transfer of hydrophobicity of polymeric insulators for various pollution severities," *International Journal of Recent Technology and Engineering*, vol. 8, no. 5, pp. 4945–4951, 2020, doi: 10.35940/ijrte.e6092.018520.
- [5] B. S. Reddy and P. C. Ramamurthy, "Analysis of in-service composite insulators used in overhead railway traction," *Engineering Failure Analysis*, vol. 108, Jan. 2020, doi: 10.1016/j.engfailanal.2019.104227.
- [6] S. Kumara and M. Fernando, "Performance of outdoor insulators in tropical conditions of Sri Lanka," *IEEE Electrical Insulation Magazine*, vol. 36, no. 4, pp. 26–35, 2020, doi: 10.1109/MEI.2020.9111097.
- [7] S. N. F. Abdullah *et al.*, "Chemical composition of rainwater harvested in East Malaysia," *Environmental Engineering Research*, vol. 27, no. 2, 2021, doi: 10.4491/eer.2020.508.
- [8] N. A. K. Abulfutouh, M. Jamie, A. Nour, and N. I. Fuad, "Rainwater harvesting quality assessment and evaluation: iium case study," *IJUM Engineering Journal*, vol. 21, no. 1, pp. 12–22, Jan. 2020, doi: 10.31436/iiumej.v21i1.1139.
- [9] M. T. Nazir *et al.*, "Simulation and experimental investigation on carbonized tracking failure of EPDM/BN-based electrical insulation," *Polymers*, vol. 12, no. 3, 2020, doi: 10.3390/polym12030582.
- [10] S. Kumagai and N. Yoshimura, "Tracking and erosion of HTV silicone rubbers and suppression mechanism of ATH," *IEEE Transactions on Dielectrics and Electrical Insulation*, vol. 8, no. 2, pp. 203–211, Apr. 2001, doi: 10.1109/94.946722.
- [11] W. Ahmed *et al.*, "Characteristics investigation of silicone rubber-based RTV/ μ ATH/ n SiO₂ micro/nano composites for outdoor high voltage insulation," *Journal of Dispersion Science and Technology*, vol. 43, no. 9, pp. 1346–1358, 2022, doi: 10.1080/01932691.2020.1857262.
- [12] R. Ullah, M. Akbar, N. Ullah, S. Al Otaibi, and A. Althobaiti, "Understanding variations in the tracking and erosion performance of htv-sr-based composites due to ac-stressed aging," *Polymers*, vol. 13, no. 21, 2021, doi: 10.3390/polym13213634.
- [13] N. N. Ali, H. Zainuddin, J. A. Razak, and R. Abd-Rahman, "Curing characteristic analysis and leakage current performances of silicone rubber via inclined plane tracking (IPT) test," in *IEEE Conference on Properties and Applications of Dielectric Materials (ICPADM)*, Jul. 2021, pp. 314–317, doi: 10.1109/ICPADM49635.2021.9493958.
- [14] A. Aman, "New leakage current parameters for newly developed polymeric composite optimized by response surface methodology," Universiti Teknologi Malaysia, 2014.
- [15] N. I. A. Majid, N. N. N. A. Malik, and N. A. Zakaria, "Beampattern optimization techniques using metaheuristic algorithm for collaborative beamforming: a review," *Bulletin of Electrical Engineering and Informatics*, vol. 12, no. 4, pp. 2185–2192, 2023, doi: 10.11591/eei.v12i4.4835.
- [16] A. A. Abubaker and Y. Y. Ghadi, "Optimization of fuzzy rules using neural network to control mobile robot in non-structured environment," *Bulletin of Electrical Engineering and Informatics*, vol. 12, no. 5, pp. 2777–2783, 2023, doi: 10.11591/eei.v12i5.5029.
- [17] B. J. Saharia and N. Sarmah, "Grey wolf optimizer for the design optimization of a DC-DC boost converter," *Bulletin of Electrical Engineering and Informatics*, vol. 12, no. 6, pp. 3263–3270, 2023, doi: 10.11591/eei.v12i6.5846.
- [18] N. N. Ali, A. Aman, J. A. Razak, Z. Zakaria, and H. Zainuddin, "Optimization of surface resistivity and relative permittivity of silicone rubber for high voltage application using response surface methodology," *Journal of Electrical Systems*, vol. Vol 13, no. 2, pp. 211–227, 2017.
- [19] F. L. Muhamedin, M. A. M. Piah, N. A. Othman, and N. Ahmed Algeelani, "Effect of contaminant flow-rate and applied voltage on the current density and electric field of polymer tracking test," *International Journal of Electrical and Computer Engineering (IJECE)*, vol. 6, no. 2, 2016, doi: 10.11591/ijece.v6i2.9517.




- [20] Seog-Hyeon Kim, E. A. Cherney, and R. Hackam, "Hydrophobic behavior of insulators coated with RTV silicone rubber," in *The 3rd International Conference on Properties and Applications of Dielectric Materials*, 1991, pp. 972–976. doi: 10.1109/ICPADM.1991.172235.
- [21] S.-H. Kim, E. A. Cherney, and R. Hackam, "Hydrophobic behavior of insulators coated with RTV silicone rubber," *IEEE Transactions on Electrical Insulation*, vol. 27, no. 3, pp. 610–622, Jun. 1992, doi: 10.1109/14.142726.
- [22] T. Sorqvist and S. M. Gubanski, "Leakage current and flashover of field-aged polymeric insulators," *IEEE Transactions on Dielectrics and Electrical Insulation*, vol. 6, no. 5, pp. 744–753, 1999, doi: 10.1109/94.798131.
- [23] Stat-Ease, "Getting started with design expert," Stat-Ease, Inc, 2013.
- [24] *Best practices capturing design and manufacturing knowledge early improves acquisition outcomes*. U.S. Government Publishing Office, 2002.
- [25] N. I. E. Service, *Total quality management*. National Industry Extension Service, 1992.

BIOGRAPHIES OF AUTHORS






Nornazurah Nazir Ali    (Ph.D. student), was born in Malaysia. She is pursuing her doctorate in Electrical Engineering (Industrial Power) at Universiti Teknikal Malaysia Melaka (UTeM). She received her degree in Electrical Engineering and an M.Sc. in Electrical Engineering from the same university in 2017. Her research interest includes high-voltage solid material (Silicone Rubber), aging of HV insulation materials, and the research processing parameters on Silicone Rubber as high-voltage insulation. She can be contacted at email: p011720003@student.utem.edu.my.






Hidayat Zainuddin    received his Bachelor's degree in electrical engineering from Universiti Teknologi Malaysia in 2003. He obtained his M.Sc. degree in electrical power engineering with Business from the University of Strathclyde, Glasgow, in 2005. He completed his Ph.D. in 2013 at the University of Southampton. In 2003, he was appointed as an academic staff member in the Faculty of Electrical Engineering, Universiti Teknikal Malaysia Melaka, and is currently the Dean of the faculty. He is a member of the official IEEE (DEIS) and IEEE (USA). His research interests include high voltage equipment and insulation condition monitoring, failure analysis, and power system protection coordination. He can be contacted at email: hidayat@utem.edu.my.



Jeefferie Abd Razak    received his Bachelor's degree from Universiti Sains Malaysia in 2004. He then pursued his master's degree and graduated with an M.Sc. in Manufacturing Engineering from Universiti Putra Malaysia. He obtained his Ph.D. in 2016 from Universiti Kebangsaan Malaysia. He is currently a senior lecturer in the Faculty of Manufacturing, Universiti Teknikal Malaysia Melaka (UTeM). His research interests mainly focus on the processing and characterization of polymer nanocomposites. He can be contacted at email: jeefferie@utem.edu.my.



Nur Farhani Ambo    received her Bachelor's in Electrical Engineering (Industrial Power) from Universiti Teknikal Malaysia Melaka in 2016. She then graduated with an M.Sc. in Electrical Engineering from the same university. She is currently serving as a lecturer at Lim Kok Wing University. Her research interests include gas discharges, high-voltage insulation systems, and measurement. She can be contacted at email: farhani.ambo@limkokwing.edu.my.